AN INVESTIGATION OF THE EFFECT OF A TURBULENT BOUNDARY LAYER UPON THE LIFT OF A WING-BODY COMBINATION WITH A GAP BETWEEN WING AND BODY AT MACH NUMBER 1.9

B. J. CARTWRIGHT AND
ROBERT C. WOOD

BOV - BOUNDARY LAYER
LIF - LIFT
TUR - TURBULENCE

AN INVESTIGATION OF THE EFFECT OF A TURBULENT BOUNDARY LAYER UPON THE LIFT OF A WING-BODY COMBINATION WITH A GAP BETWEEN WING AND BODY AT MACH NUMBER 1.9

by

LT B. J. CARTWRIGHT, USN

and

LT ROBERT C. WOOD, USN

Performed at the

UNIVERSITY OF MICHIGAN

as part of the third year curriculum of the

U. S. NAVAL POSTGRADUATE SCHOOL

Monterey, California

1 MAY 1955

AN INVESTIGATION OF THE EFFECT OF A TURBULENT BOUNDARY LAYER UPON THE LIFT OF A WING-BODY COMBINATION WITH A GAP BETWEEN WING AND BODY AT MACH NUMBER 1.9

SUMMARY

There have been several theoretical investigations which predict the effects of a gap between the wing and body upon the lift of the wing-body combination. In this investigation, the theoretical predictions of the lift variation with gap, for a given model, are corrected for the displacement thickness due to a turbulent boundary layer in the gap. These results are then compared with the experimental lift variation of the model.

The loss in lift due to a gap as determined experimentally, for gap widths greater than the boundary layer thickness, is much less than that predicted by theory. The corrections to the theoretical predictions made by reducing the gap by the displacement thickness are so small that they fail in large measure to explain the great difference between experiment and theory.

The results of lift variation with gap for gap widths less than the boundary layer thickness are uncertain and this area of the gap problem is recommended for further investigation.

SYMBOLS

a	speed of sound
C_p	specific heat at constant pressure
g	gap width between wing and body
H	δ^*/θ , boundary layer shape parameter
k	thermal conductivity
$\frac{L}{L_{g=0}}$	ratio of lift with gap to the lift without gap
M	Mach number
n	denominator of exponent describing velocity profile, ie. $u/u_1 - (y/\delta)^{1/n}$)
p	static pressure
p_t	total pressure
r_o	radius of model body
S_o^*	wing body semi-span with no gap
T	absolute temperature
$\frac{g}{g + S_o^*}$	gap parameter
u	velocity component in boundary layer parallel to the free stream flow direction
V	speed of flow
x	streamwise direction
y	Height above surface perpindicular to the surface
α	angle of attack
γ	ratio of specific heats, C_p/C_v
δ	boundary layer thickness
δ^*	boundary layer displacement thickness

θ	boundary layer momentum thickness
ρ	mass density
μ	absolute viscosity

Subscripts

1	refers to conditions ahead of the normal shock wave or to the conditions at the edge of the boundary layer
2	refers to conditions behind the normal shock wave
c	refers to values corrected for δ^*
t	refers to total or stagnation conditions
∞	refers to remote conditions
1/7	refers to the velocity profile, $u/u_1 = (y/\delta)^{1/7}$
1/4.83	refers to the velocity profile, $u/u_1 = (y/\delta)^{1/4.83}$
cal	refers to values calculated from theory
obs	refers to values calculated from experiment

AN INVESTIGATION OF THE EFFECT OF A TURBULENT BOUNDARY LAYER UPON THE LIFT OF A WING-BODY COMBINATION WITH A GAP BETWEEN WING AND BODY AT MACH NUMBER 1.9

INTRODUCTION

With the more frequent use of all movable control surfaces on guided missles and high-performance aircraft, it has become of some interest to determine the effects upon lift of a gap between the wing and body. There have been several theoretical investigations such as Ref. 1, to determine these effects. Such theoretical attempts have, of necessity, ignored the effects of a boundary layer in the gap. The present investigation is an attempt to determine experimentally the effect of a turbulent boundary layer on a wing-body combination with gap in supersonic flow and compare it with the theoretical predictions of Ref. 1.

The method of analysis is to first determine the boundary layer displacement thickness from the measured velocity profile. The theoretical calculation of the lift on the body with the measured gap versus the theoretical lift on the body with the gap reduced by the displacement thickness can then be compared with the changes in lift actually measured.

The experimental measurements of the changes in lift were taken from Ref. 2, which was an investigation carried out simultaneously with this one at the same Mach number

and with the same model in several configurations, including the configuration used in this report.

The determination of the boundary layer displacement thickness in an asymmetric flow is complex and beyond the scope of this investigation. Of necessity, the body and wings were restricted to a zero degrees angle of attack.

This investigation was conducted by LT B. J. Cartwright, USN, and LT Robert C. Wood, USN, during January and February, 1955, at the Supersonic Wind Tunnel, University of Michigan, Ann Arbor, Michigan, as part of the third year curriculum in Aeronautical Engineering of the U. S. Naval Postgraduate School, Monterey, California. The project was financed by the Bureau of Aeronautics, Navy Department, Washington, D.C.

The authors are especially indebted to Arnold M. Kuethe, Felix Pawlowski Professor of Aerodynamics, University of Michigan, and to H. P. Liepman, Director, Supersonic Wind Tunnel, University of Michigan, for their guidance and advice in the course of the investigation. Grateful acknowledgement is also made to LT J. F. Ahearn, USN, LT K. B. Mattson, USN, and to the members of the Wind Tunnel Staff for their help and assistance.

EQUIPMENT AND PROCEDURE

The experimental work was performed in the University of Michigan 3 inch by 13 inch Supersonic Wind Tunnel, Mach 1.9 channel. A complete description of this facility is contained in Ref. 3.

Description of Model

The model consists of a cone cylinder with swept wings as shown in Fig. 1 a. A photograph of the model mounted in the test section of the wind tunnel is shown in Fig. 2.

The body has a diameter of 1.055 inches and an over-all length of 9.117 inches. The nose of the body is a cone 2.992 inches in length with a semi-vertex angle of 10 degrees.

The delta shaped wings measure 1.548 inches from tip to root and have a leading edge sweep-back angle of 35.75 degrees. To permit a gap between wing and body, the wings are attached to the body by means of a pin which fits into a bushing in the body. In order to withstand any transient loads on the wing, which might occur during starting or stopping the tunnel, a maximum pin diameter of 0.185 inches was used. The arrangement is such that the leading edge of the wing at the root is 1.350 inches behind the shoulder of the nose cone. The gap between wing and body was set at 0.155 inches.

To insure a turbulent boundary layer, a small wire ring

is fixed to the nose of the cone to act as a boundary layer tripring device. The ring is made of wire having a .0055 inch diameter and is located 1.323 inches ahead of the shoulder of the cone.

Boundary Layer Survey Equipment

The boundary layer velocity profile was determined by pressure measurements with the total head probe shown in Fig. 1 b. The probe was constructed of stainless steel hypodermic tubing with an outside diameter of 0.042 inches. This tubing was flattened and stoned to an elliptic shape with 0.0127 by 0.0680 inches outside dimensions and 0.0063 by 0.0600 inches inside dimensions. With the probe against the body, the center of the orifice was 0.1375 mm. (0.0054 inches) above the body. The tubing was then soldered into 0.125 inch copper tubing and ground and buffed to a streamlined shape. The response time of the probe is six seconds.

The boundary layer survey was made in the gap at a point even with the leading edge of the wing at its root. To traverse the boundary layer, the after part of the probe was securely taped to the after-body of the model with shims inserted between the probe and the model to give the desired height of the probe orifice above the body. This allowed only one height to be used during each run.

This height was determined by arc measurement with a Wild T-2 universal theodolite. The theodolite can normally

be read accurately to one second of arc. It was placed 11.4 feet from the model, this distance being measured to a minimum accuracy of 1/8 inches. The vibration of the probe with the tunnel running somewhat lessened the normal accuracy of the theodolite readings. Another source of error was the refraction of the light waves due to the density gradients in the boundary layer. The magnitude of this error was small, as indicated by measurements of the model body with and without the tunnel running.

With these factors, the consistant accuracy of the arc measurements was within 8 seconds of arc, corresponding to 0.005 inches in the probe height.

The pressures were measured with mercury manometers which were read to the nearest 0.01 inches of mercury.

Several Schlieren photographs were taken, one of which is shown in Fig. 3. Upon enlargement, the Schlierens showed the wavy fringe that typifies the edge of a turbulent boundary layer.

Experimental procedure and Data Reduction

Prior to each run, theodolite readings were taken of the body and the probe. Readings of the theodolite and manometers were taken during the run after the flow field and manometers had stabilized.

In accordance with standard procedure for this wind tunnel, the remote stagnation pressure, p_{t_∞}, was taken as

the barometric pressure. The manometer readings were corrected for the difference in manometer and barometric temperatures.

As a check on the free stream Mach number for each run, a reading was made of the static pressure on the floor of the tunnel 0.65 inches forward of the nose of the model.

The determination of the velocity from the total head probe readings was made using the tables of Ref. 4. The relations used are as follows.

For a blunt total head probe in a supersonic flow, the pressure measured is that behind a normal shock wave. The ratio of total pressures ahead of and behind the normal shock can be expressed as a function of the Mach number ahead of the shock by the following equation (see Symbols):

$$\text{Eq.(1)} \qquad \frac{p_{t_2}}{p_{t_1}} = \left[\frac{(\gamma+1)\,M_1^2}{(\gamma-1)\,M_1^2+2}\right]^{\frac{\gamma}{\gamma-1}} \left[\frac{\gamma+1}{2\gamma M_1^2-(\gamma-1)}\right]^{\frac{1}{\gamma-1}}$$

The Rayleigh pitot formula relates the ratio of the upstream static pressure and the stagnation pressure behind the normal shock wave to Mach number as follows:

$$\text{Eq.(2)} \qquad \frac{p_{t_2}}{p_1} = \left[\frac{\gamma+1}{2} M_1^2\right]^{\frac{\gamma}{\gamma-1}} \left[\frac{\gamma+1}{2\gamma M_1^2-(\gamma-1)}\right]^{\frac{1}{\gamma-1}}$$

The ratio of velocity to the stagnation speed of sound is given by:

$$\text{Eq.(3)} \qquad \frac{V}{a_t} = M^2\left(1+\frac{\gamma-1}{2}M^2\right)^{-1}$$

These three equations are valid for the adiabatic flow of a perfect fluid.

The customary additional assumptions in determining the velocity profile and the displacement thickness are:

(1) The static pressure is constant through the boundary layer.

(2) The Prandtl number is unity.

(3) The thermal conductivity, k, and the absolute viscosity, μ, are constant through the boundary layer.

(4) No heat is transferred through the surface of the model, ie., an insulated surface.

(5) The velocity profile of the turbulent boundary layer obeys a power law, $u/u_1 = (y/\delta)^{1/n}$.

To these was added an additional assumption that

(6) The loss in total pressure across the conical shock wave for a nose cone of a semi-vertex angle of 10 degrees is negligible.

By the latter assumption $p_{1t} = p_{t_\infty}$

This assumption was originally based on Ref. 5, which has condensed some of the conical shock wave data from Ref. 6 into convenient charts and curves, one of which plotted the stagnation pressure ratio across conical shock waves versus Mach number for various cone angles. This curve, readable to three decimal places, indicated a negligible pressure loss across the shock wave for this nose cone.

To check the validity of the assumption of a negligible

pressure loss across the shock waves and to obtain the local static pressure, three preliminary runs were made with the total head probe outside the boundary layer and with a needle static pressure probe located on the body with its orifice diametrically opposite to the total head probe.

The measured static pressures were compared with the static pressures calculated using the barometric pressure as p_{t_1}.

Since the quantities p_{t_2}/p_{t_1} and p_1/p_{t_2} are tabulated in Ref. 4 from equations (1) and (2), the calculation consisted of merely entering the tables with p_{t_2}/p_{t_1} and obtaining the corresponding p_1/p_{t_2}. Then

$$p_1 = (p_1/p_{t_2})\, p_{t_2}$$

The calculated static pressure and the values measured with the static pressure probe are recorded in Table I. They compare closely and support the assumption of a negligible pressure loss across the shock waves.

Since the barometer, and therefore p_{t_1}, was seldom constant during the investigation, the first, and if possible the last of the runs for each day were made with the total head probe in the free stream outside the boundary layer. The static pressure was then calculated as illustrated above.

Since the velocity ratio, V/a_t given by equation (3) is also tabulated versus Mach number, the velocity ratio at the edge of the boundary layer u_1/a_t was simultaneously determined.

The velocity ratio, u/a_t, in the boundary layer was obtained by entering the tables with p_1/p_{t_2}, p_1 being that from the free stream run or an average of the free stream runs during the day, and obtaining u/a_t directly. Then

$$\frac{u}{u_1} = \frac{(u/a_t)}{(u_1/a_t)}$$

These values are tabulated in Table I.

Preliminary rectangular and logarithmic plots were made of the velocity profile to determine the boundary layer thickness, δ. The edge of the boundary layer was taken where $u/u_1 = 0.994$ from which

$$\delta = 1.2 \text{ mm.} = 0.0472 \text{ inches}$$

The non-dimensional logarithmic plot and velocity profile are shown in Figs. 4 and 5.

The two-dimensional displacement thickness is customarily defined from the equation

$$\int_0^{\delta} \rho u \, dy = \int_{\delta^*}^{\delta} \rho_1 u_1 \, dy$$

or

Eq.(4) $$\delta^* = \int_0^{\delta} \left(1 - \frac{\rho u}{\rho_1 u_1}\right) dy$$

For steady two-dimensional flow, it is shown in Ref. 7 that the energy equation reduces to

$$\rho C_p \left(u \frac{\partial T}{\partial x} + v \frac{\partial T}{\partial y}\right) - u \frac{\partial p}{\partial x} = \frac{\partial}{\partial y}\left(k \frac{\partial T}{\partial y}\right) + \mu \left(\frac{\partial u}{\partial y}\right)^2$$

For assumptions (2), (3) and (4), a solution to the energy equation is

$$C_p T + \tfrac{1}{2} u^2 = C_p T_1 + \tfrac{1}{2} u_1^2$$

This may be written

Eq.(5) $$\frac{T}{T_1} = 1 + \frac{\gamma - 1}{2} M_1^2 \left[1 - (u/u_1)^2 \right]$$

By assumptions (1) and (5)

Eq.(6) $$\rho_1/\rho = T/T_1$$

Eq.(7) $$u/u_1 = (y/\delta)^{1/n}$$

Substituting equations (5), (6), and (7) into equation (4) yields

Eq.(8) $$\delta^* = \delta \int_0^1 \left\{ 1 - \frac{(y/\delta)^{1/n}}{1 + \frac{\gamma - 1}{2} M_1^2 \left[1 - (y/\delta)^{2/n} \right]} \right\} d(y/\delta)$$

The integrand of this equation was calculated for 21 points over the interval and the integration was carried out graphically.

DISCUSSION AND RESULTS

Boundary Layer Velocity Profile

The equation of the velocity profile was determined to be

$$u/u_1 = (y/\delta)^{1/n} = (y/\delta)^{1/4.83}$$

The boundary layer displacement thickness was found to be

$$\delta^* = 0.365 \text{ mm.} = 0.0144 \text{ inches}$$

An adverse pressure gradient exists on the model aft of the shoulder due to the expansion. This pressure distribution is shown for a similar model in Fig. 6. (Ref. 8)

No quantitative data appeared available correlating boundary layer profiles with adverse pressure gradients for compressible flows. Perhaps this is due to the difficulty in accurately making such measurements without shock wave interference. However, R. E. Wilson, in his work on the growth of the turbulent boundary layer, (Refs. 9 and 10) for zero and favorable pressure gradients in compressible flow, has correlated the boundary layer shape parameter, $H = \delta^*/\theta$, with the Mach number outside the boundary layer. For his tabulations, Wilson chose a 1/7 power law for the velocity profile. This selection, he explains, was because a 1/7 power law has been used at subsonic speeds and has been found to apply for the boundary layer on a flat plate at supersonic speeds for a moderate range of Reynold's numbers.

To determine the shape parameter, the momentum thickness was calculated using the assumptions previously mentioned. The equation is

Eq. (9) $\theta = \delta \int_0^1 \frac{\rho u}{\rho_1 u_1} \left(1 - \frac{u}{u_1} \right) \quad d(y/\delta)$

From which

$\theta_{1/4.83} = 0.1086$ mm. $= 0.00428$ inches

A 1/7 power profile is also shown in Fig. 5. Calculation of the displacement and momentum thicknesses for the 1/7 profile by the methods above gave

$\delta^* = 0.289$ mm $= 0.0114$ inches

$\theta_{1/7} = 0.09096$ mm $= 0.00358$ inches

The Mach number at the edge of the boundary layer at the survey station was 2.032. For this value and a 1/7 power law, Ref. 10 tabulates

$H_{1/7} = 3.131$

From the above calculations the shape parameters were

$H_{1/7} = 3.171$

$H_{1/4.83} = 3.361$

This comparison of shape parameters is considered quite favorable. The numerical values compare closely with the experimental profile having the largest value. Since, other things being equal, the larger values of shape parameter correspond to boundary layers more nearly to the separation point, the effect of an adverse pressure gradient should be reflected in a higher value of H.

Also, the character of the change in the exponent, n, is

in a direction consistant with Clauser's work in incompressible flow with an adverse pressure gradient. (Ref. 11)

The probe effects and the interference effects due to the presence of the pin, the tape, and the reflected shock waves in the gap are unknown and were neglected.

Effects of Displacement Thickness

The authors of Ref. 1, Dugan and Hikido, in their linearized inviscid theory, have developed the variation of lift due to gap width as a function of a gap parameter, $\frac{g}{g + S_o^*}$, where g is the width of the gap and S_o^* is the wing-body semi-span with no gap.

The lift versus gap parameter curves were presented for values of r_o/S_o^* of 0.500 and 0.216. The value of r_o/S_o^* for the model used in this investigation is 0.254. A curve for this value was derived from linear interpolation of the other two curves and is shown in Fig. 7.

The corresponding experimental curve of the lift variation with gap parameter was developed in Ref. 2. This is also shown in Fig. 7.

Since the effect of the displacement thickness on the lift variation decreases as the gap increases, the curves are shown only for the range of gap parameter from 0 to 0.14. The effects of δ^* will first be considered for gap parameters corresponding to gap widths greater than the boundary layer thickness.

The determination of a boundary layer displacement thick-

ness in this investigation was, of necessity, limited to two-dimensional flow at a zero angle of attack. The effect of an angle of attack would be to add a cross-flow component and would of course involve a three-dimensional displacement thickness. To evaluate these effects, however, reference was made to Moore's work on compressible laminar boundary layer flow in Refs. 12, 13, and 14. Although Moore doesn't deal explicitly with a cone cylinder, his determinations of the displacement effect on yawed circular cones and yawed infinite cylinders at the plane 90 degrees from the stagnation line at small angles of attack would indicate a tendency for a small decrease in the displacement thickness. Projecting this to the turbulent boundary layer in this case, it was assumed that there would be a very small decrease, negligible for this report, in the displacement thickness from the two-dimensional case at the position of the wing for angles of attack up to 10 degrees, the range considered in Ref. 2. However, there is no experimental data to substantiate this assumption.

To determine the effects of the displacement thickness on lift from the theoretical predictions, the value of the lift ratio, $L/L_{g=0}$, at a given gap parameter, was compared with the lift ratio for a gap reduced by the displacement thickness, ie., for a gap parameter of $\frac{g - \delta^*}{(g - \delta^*) + S_o^*}$. These values were then compared with the experimental values, Fig.7. If the only deviations of experiment from theory were due to

the boundary layer displacement thickness, these values would, of course, coincide.

The values are tabulated in Table II. To better illustrate the comparison, Fig. 8 shows the percentage increase of the lift ratio predicted by Ref. 1 due to a reduction in the gap width by δ^*. A second curve shows the percentage increase of the experimental lift ratios over the theoretical values.

Table II and Fig. 8 show that the displacement thickness has a relatively small effect on the lift variation for gap widths greater than the boundary layer thickness. The change in lift is shown to vary from 0% at a gap parameter of .14 to 4.0% at a gap parameter corresponding to the boundary layer thickness. The percentage of the experimental values over the theoretical values is shown to vary from 70.3% to 62.0% over the same range. Therefore, correcting the theoretical predictions for a displacement thickness accounts for only a small part of the difference in experiment and theory. Thus the concept of a boundary layer displacement thickness (or displacement surface in this case) fails in large degree to explain the big difference in the experimental values and the theoretical values of the lift variation with gap. Large errors in the displacement thickness calculations would still fail to account for the major part of this difference. For instance, tripling the displacement thickness at a gap parameter of 0.05 would only correct the theoretical predictions

by 7.5% compared with a 67% difference between the measured lift ratio and that predicted by theory. The greater part of the difference must therefore be attributed to other factors. Some possibilities for these other factors are the linearization of the equations in Ref. 1, the deviation of the model from the slender body requirement, other viscous effects not considered, such as the boundary layer on the surface of the wing root, the presence of the pin in the gap, and compressibility effects.

Consideration was next given to the range of gap widths less than the boundary layer thickness. Bleviss and Struble in Ref. 15, and others, have indicated a belief that the effects of viscosity are such as to cause an inflection in the lift ratio versus gap curve at very small gaps so that the curve approaches unity somewhat asymptotically, as shown in Fig. 7. If the displacement surface was a real surface instead of an artificial one, the lift ratio would, of course, reach unity at a gap corresponding to δ^*. However, it is anticipated that even at this gap width there would be some small flow through the gap.

In an attempt to check the inflection in the lift ratio curve, additional runs were made at a gap width equal to δ^*. The runs were made using newly installed automatic data reduction equipment and the results were as follows:

$$\alpha = 5^\circ, \ \frac{L}{L_{g=0}} = 1.112 \quad ; \ \alpha = 10^\circ, \ \frac{L}{L_{g=0}} = 1.119$$

It is considered highly improbable that the lift ratio increases even for gap widths between zero and σ^*. The accuracy of the above results is therefore questionable. The wind tunnel test schedule did not permit the necessary reruns to check these results. This area of the gap effects problem is considered of high interest, however, and is recommended as warranting more extensive investigation.

CONCLUSIONS AND RECOMMENDATIONS

The following conslusions and recommendations can be drawn from the results of this investigation:

1. The experimental data of Ref. 2 indicates the loss in lift due to a gap between wing and body to be much less than predicted by Ref. 1. The concept of a displacement surface due to a turbulent boundary layer in the gap, fails in large measure to account for this difference for gap widths greater than the boundary layer thickness.

2. The results of an attempt to determine the lift ratio at a gap width corresponding to the displacement thickness are uncertain and the region of gap widths less than the boundary layer thickness is therefore recommended for further investigation.

REFERENCES

1. Dugan, D. W., and Hikido, H.: Theoretical Investigation of the Effects Upon Lift of a Gap Between Wing and Body of a Slender Wing-Body Combination. NACA TN 3224, August 1954.
2. Ahearn, J. F., and Mattson, K. B.: Experimental Investigation of the Effects Upon Lift of a Gap Between Wing and Body of a Wing-Body Combination at Mach Number 1.9. Thesis, U.S. Naval Postgraduate School, May 1955.
3. Garby, L. C., and Nelson, W. C.: University of Michigan 8x13 inch Intermittent-Flow Supersonic Wind Tunnel. University of Michigan Memorandum No. 59, Engineering Research Institute, June 1950.
4. Ames Research Staff: Equations, Chart Tables, and Charts For Compressible Flow. NACA Report 1135, 1953.
5. Dailey, C. L., and Wood, F. C.: Computation Curves for Compressible Fluid Problems. John Wiley and Sons, Inc., New York, 1949.
6. Mass. Inst. of Tech., Dept of Elect. Eng., Center of Analysis. Tables of Supersonic Flow Around Cones by the Staff of the computing Section under the direction of Zdenek Kopal Tech Rep. no. 1 Cambridge, 1947.
7. Howarth, L.: Modern Developments in Fluid Dynamics, High Speed Flow. Oxford at The Clarendon Press, Great Britain, 1953.

8. Clark, E. T.: Pressure Measurements on the Pressure Model P2,0, WTM-164 June 7, 1950, Supersonic Wind Tunnel, University of Michigan.

9. Wilson, R. E., Young, E. C. and Thompson, M. J.: 2nd Interim Report on Experimentally Determined Turbulent Boundary Layer Characteristics at Supersonic Speeds, DRL/UT Report CM-501, DRL-196, (25 January 1949).

10. Wilson, R. E.: Turbulent Boundary Layer Growth With Favorable Static Pressure Gradient at Supersonic Speeds, reprinted from the Proceedings of The Second Midwestern Conference on Fluid Mechanics by Ohio State University, 1952.

11. Clauser, Francis H.: Turbulent Boundary Layers in Adverse Pressure Gradients. Jour. Aero. Sci., Vol. 21, no. 2, February 1954, pp. 91 - 108.

12. Moore, Franklin K.: Three Dimensional Compressible Laminar Boundary-Layer Flow. NACA TN 2279, March 1951

13. Moore, Franklin K.: Laminar Boundary Layer on a Circular Cone in Supersonic Flow at a Small Angle of Attack. NACA TN 2521, October 1951.

14. Moore, Franklin K.: Displacement Effect of a Three-Dimensional Boundary Layer. NACA TN 2722, June 1952.

15. Bleviss, Z. O., and Struble, R. A.: Some Aerodynamic Effects of Streamwise Gaps in Low-Aspect-Ratio Lifting Surfaces at Supersonic Speeds. IAS Preprint No. 396, 1953.

TABLE I

BOUNDARY LAYER SURVEY DATA

RUN NO.	y mm.	$p_{cal.}$ in.Hg	$p_{obs.}$ in.Hg	p_{t_2} in.Hg	u/a_a	u_1/a_a	u/u_1	y/δ
1	4.3949	3.68	3.70	21.24	- -	1.4997	1.0000	3.655
2	4.4152	3.64	3.67	21.15	- -	1.5030	1.0000	3.668
3	4.3882	3.68	3.68	21.26	- -	1.5020	1.0000	3.658
4	2.4006	3.57	- -	20.72	- -	1.5040	1.0000	2.000
5	0.1375	3.57	- -	7.47	0.9752	1.5040	0.6484	0.114
6	0.1375	3.57	- -	7.11	0.9453	1.5040	0.6285	0.114
7	0.4637	3.57	- -	12.01	1.2380	1.5040	0.8231	0.386
8	1.4271	3.57	- -	20.53	1.5000	1.5040	0.9973	1.189
9	0.8000	3.57	- -	16.18	1.3880	1.5040	0.9229	0.667
10	0.6361	3.57	- -	13.79	1.3090	1.5040	0.8703	0.530
11	1.4676	3.48	- -	20.42	- -	1.5090	1.0000	1.222
12	0.4874	3.48	- -	12.04	1.2520	1.5090	0.8297	0.406
13	0.3336	3.48	- -	9.83	1.1450	1.5090	0.7588	0.278
14	0.6310	3.48	- -	12.51	1.2720	1.5090	0.8429	0.526

TABLE II

LIFT VARIATION WITH GAP

THEORITICAL						OBSERVED	
			CORRECTED FOR σ^*				
$\frac{g}{g + S_o^*}$	$\frac{L}{L_{g=0_{cal}}}$	g in.	$\frac{g - \sigma^*}{g-\sigma^*+S_o^*}$	$\frac{L}{L_{g=0_c}}$	%	$\frac{L}{L_{g=0_{obs}}}$	%
0	1.000	0	- -	- -	- -	- -	- -
.01	.617	.0210	.0031	.670	8.6	.958	55.3
.02	.575	.0424	.0133	.600	4.4	.926	61.0
.03	.549	.0642	.0234	.565	2.9	.900	63.9
.04	.530	.0865	.0336	.542	2.3	.880	66.0
.05	.514	.1092	.0437	.524	2.0	.860	67.3
.06	.502	.1325	.0538	.509	1.4	.843	67.9
.07	.491	.1562	.0640	.498	1.3	.826	68.2
.08	.481	.1805	.0741	.487	1.2	.813	68.9
.09	.472	.2053	.0842	.477	1.2	.801	69.7
.10	.462	.2306	.0943	.467	1.1	.788	70.0
.11	.454	.2565	.1045	.458	0.8	.775	70.6
.12	.447	.2830	.1146	.450	0.8	.763	70.5
.13	.441	.3101	.1247	.444	0.7	.752	70.4
.14	.435	.3379	.1400	.435	0	.741	70.4

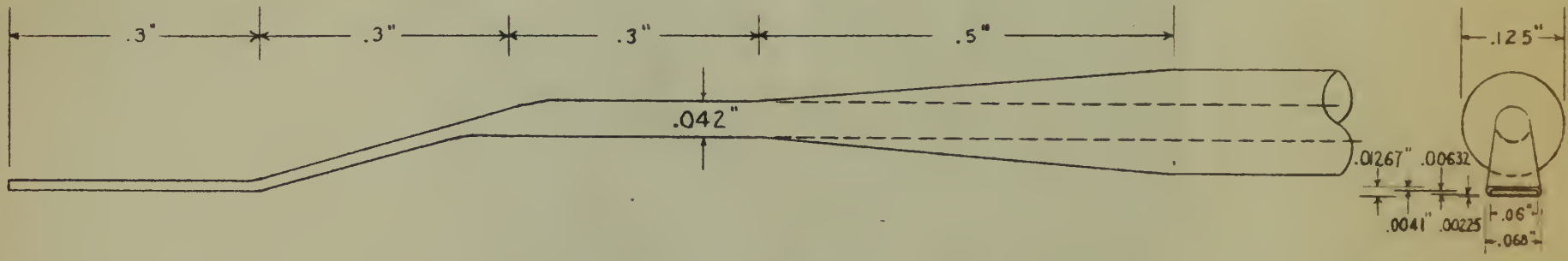

FIG. 1b
PROBE

FIG. 1a MODEL

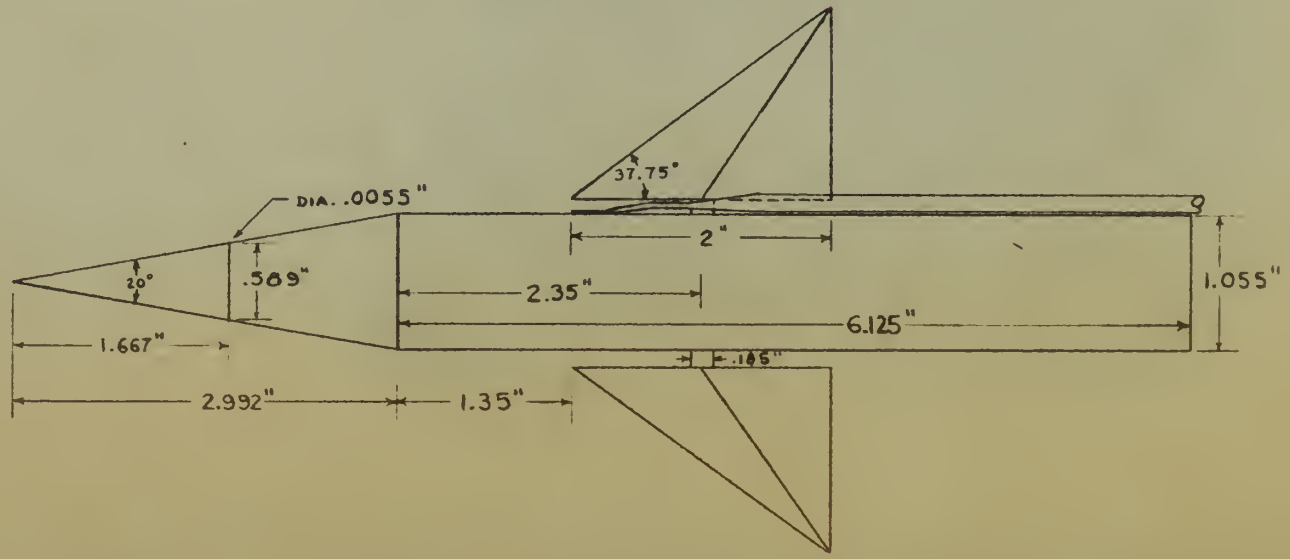

FIG. 2

MODEL MOUNTED IN TUNNEL TEST SECTION WITH PROBE ATTACHED

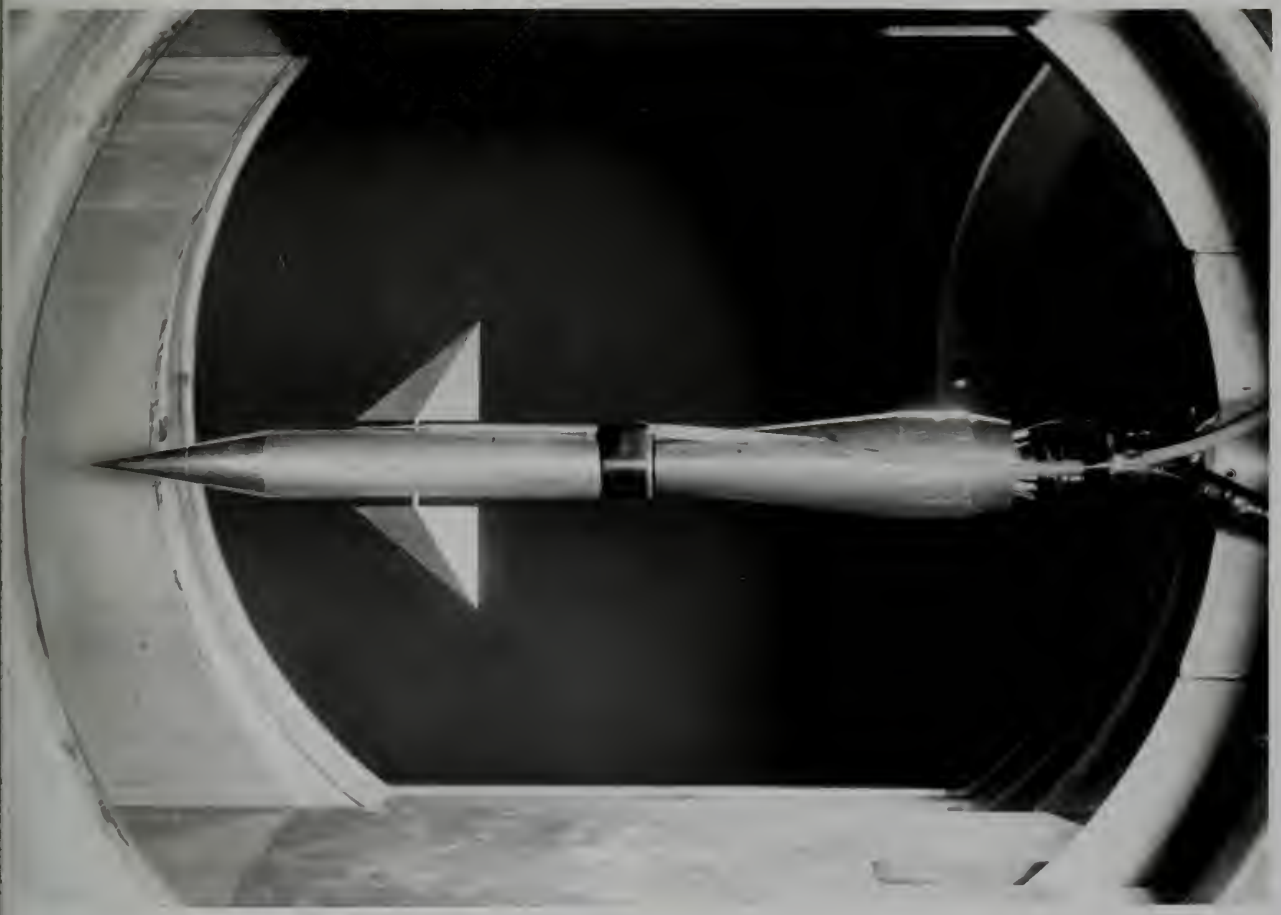

FIG. 3

SCHLIEREN PHOTOGRAPH OF MODEL

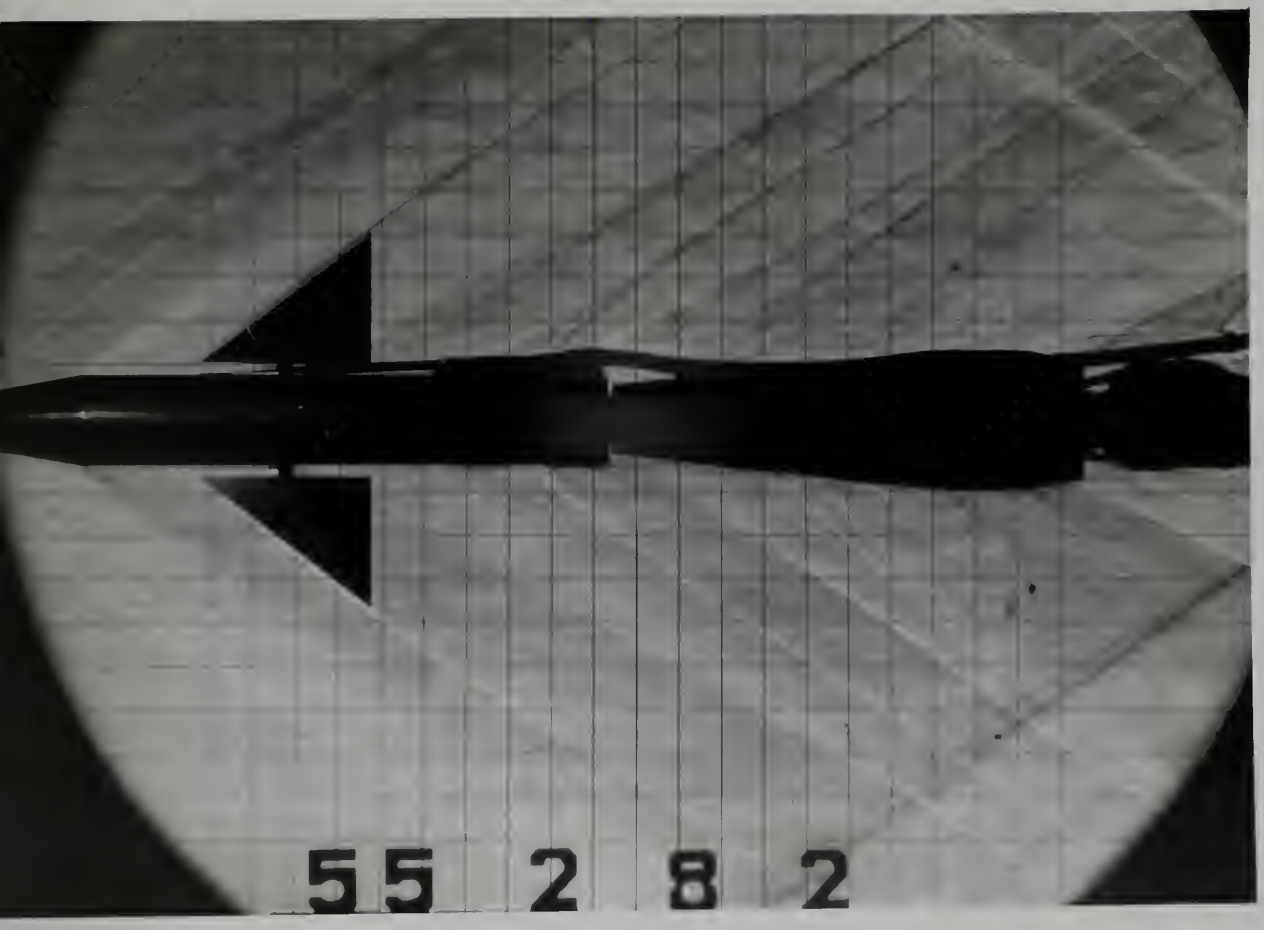

FIG. 4

PLOT FOR THE DETERMINATION OF THE PROFILE POWER

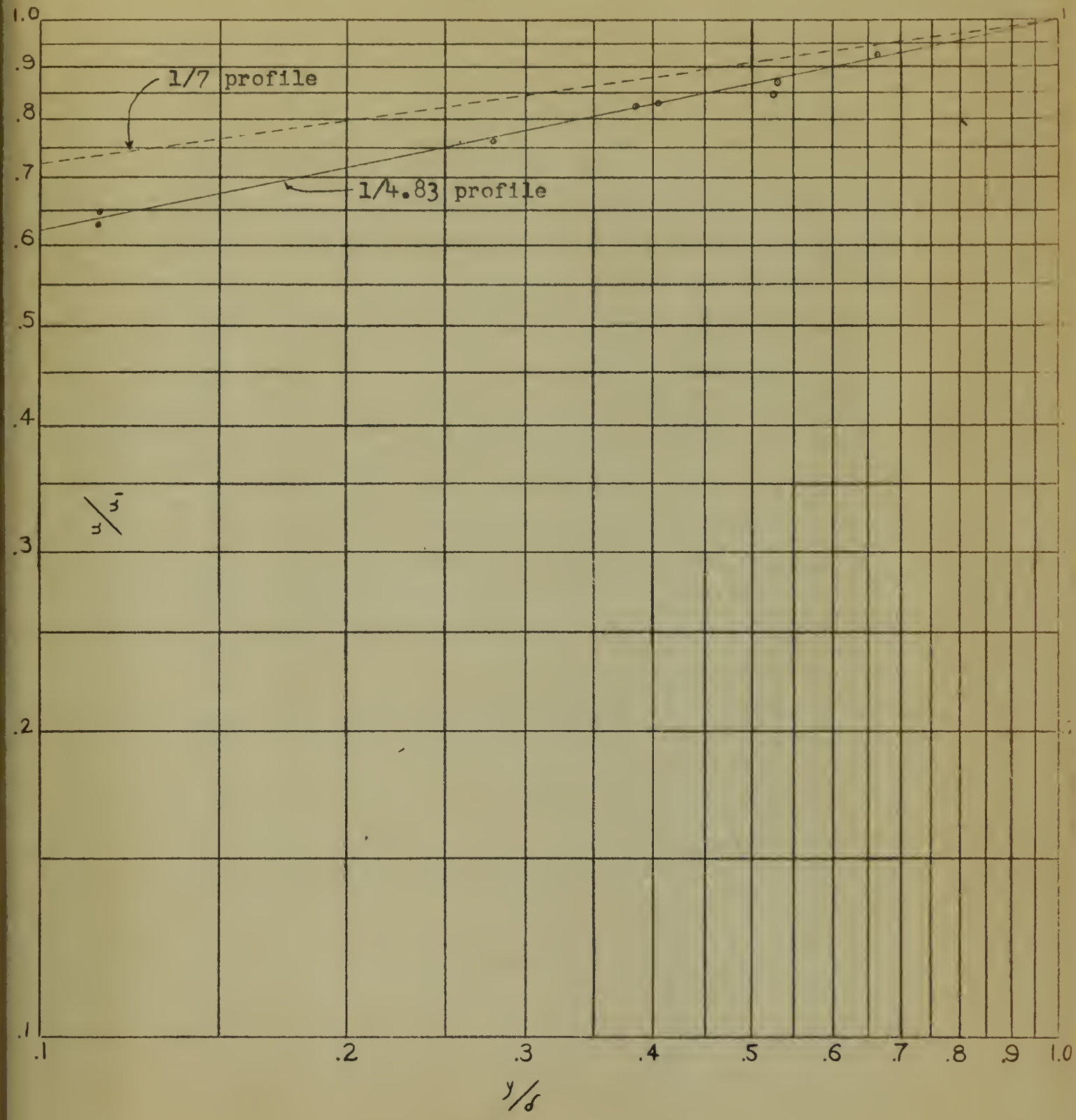

FIG. 5

VELOCITY PROFILE

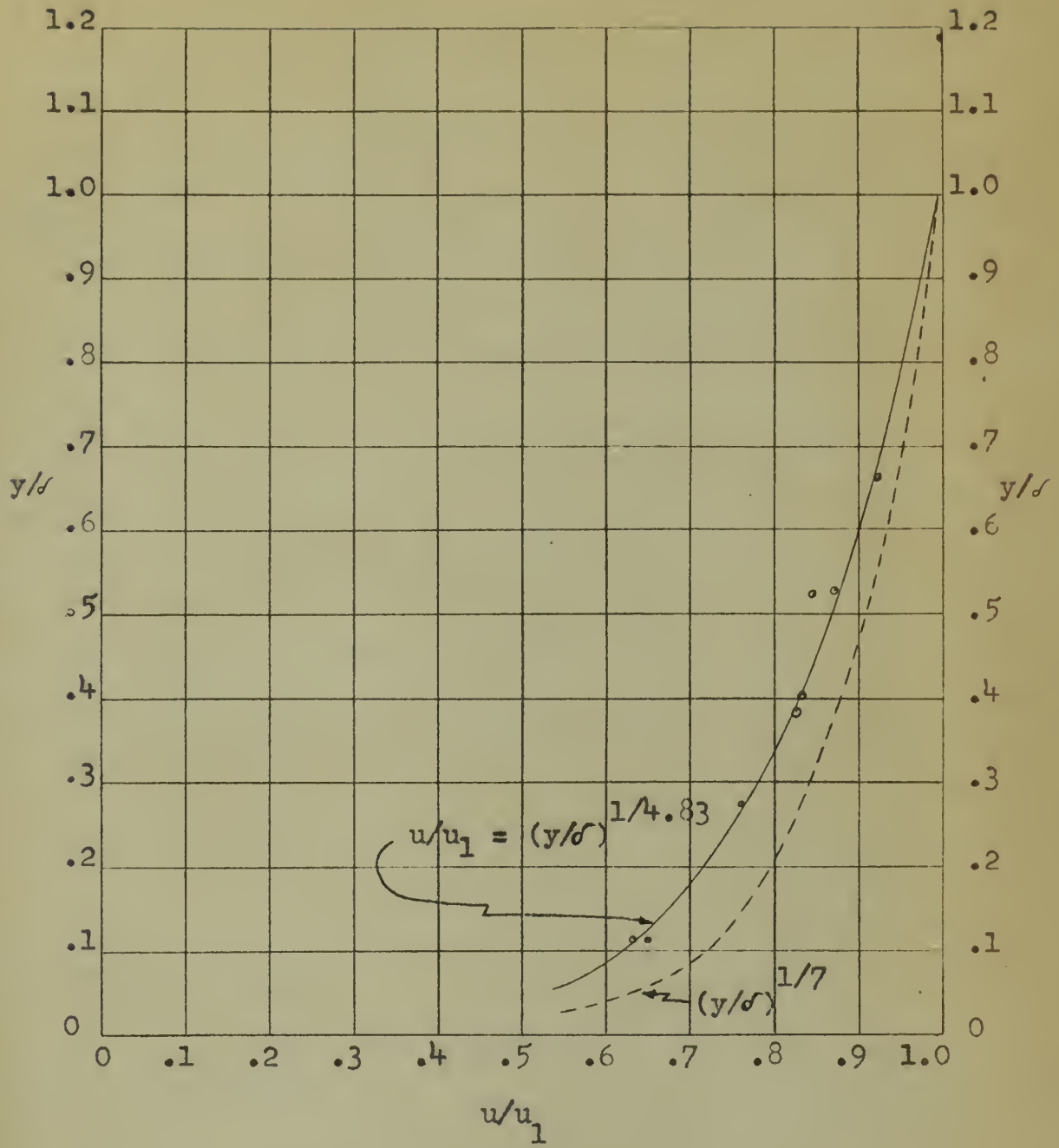

FIG. 6

PRESSURE DISTRIBUTION ABOUT A CONE CYLINDER

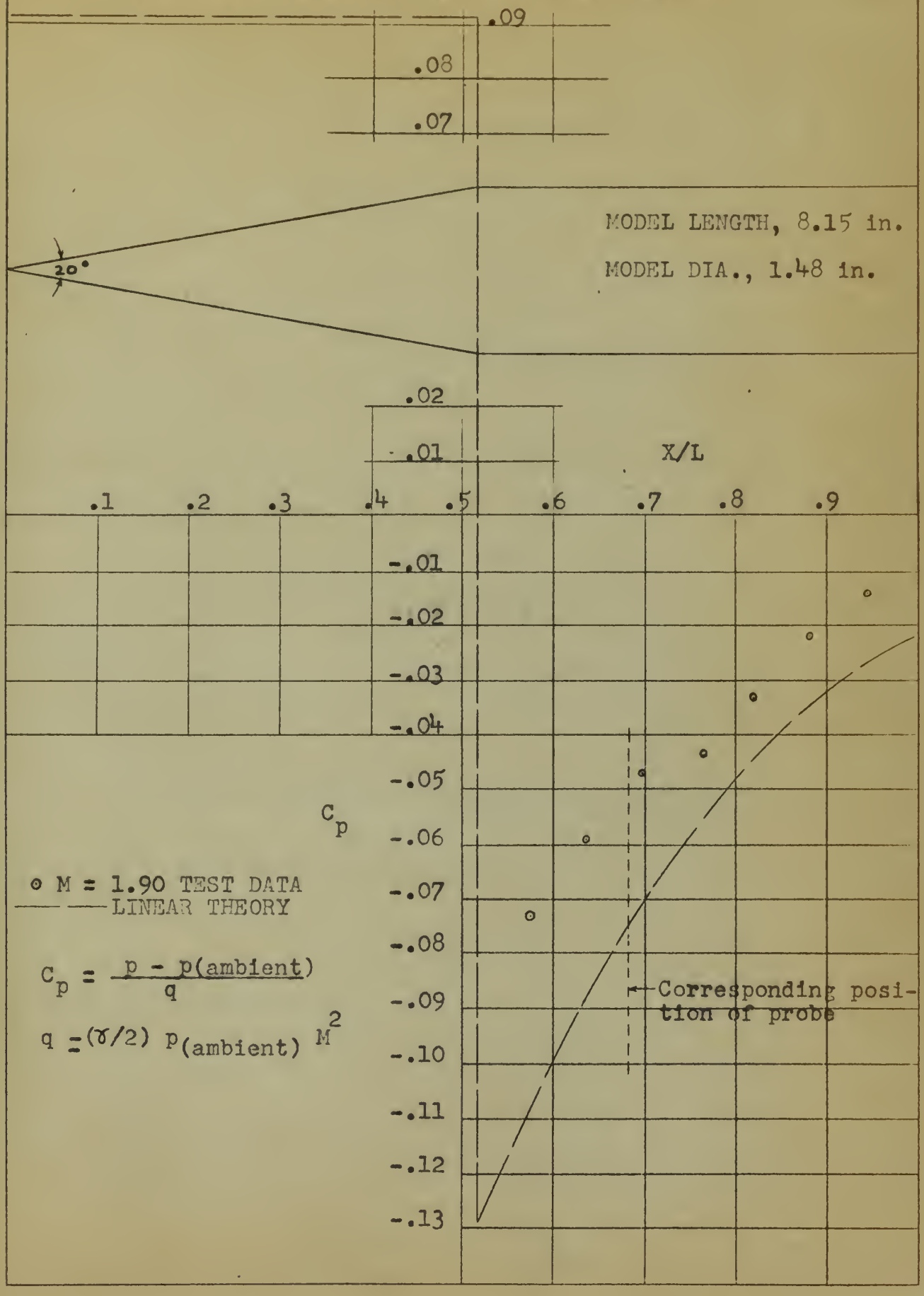

FIG. 7

LIFT RATIO VERSUS GAP PARAMETER

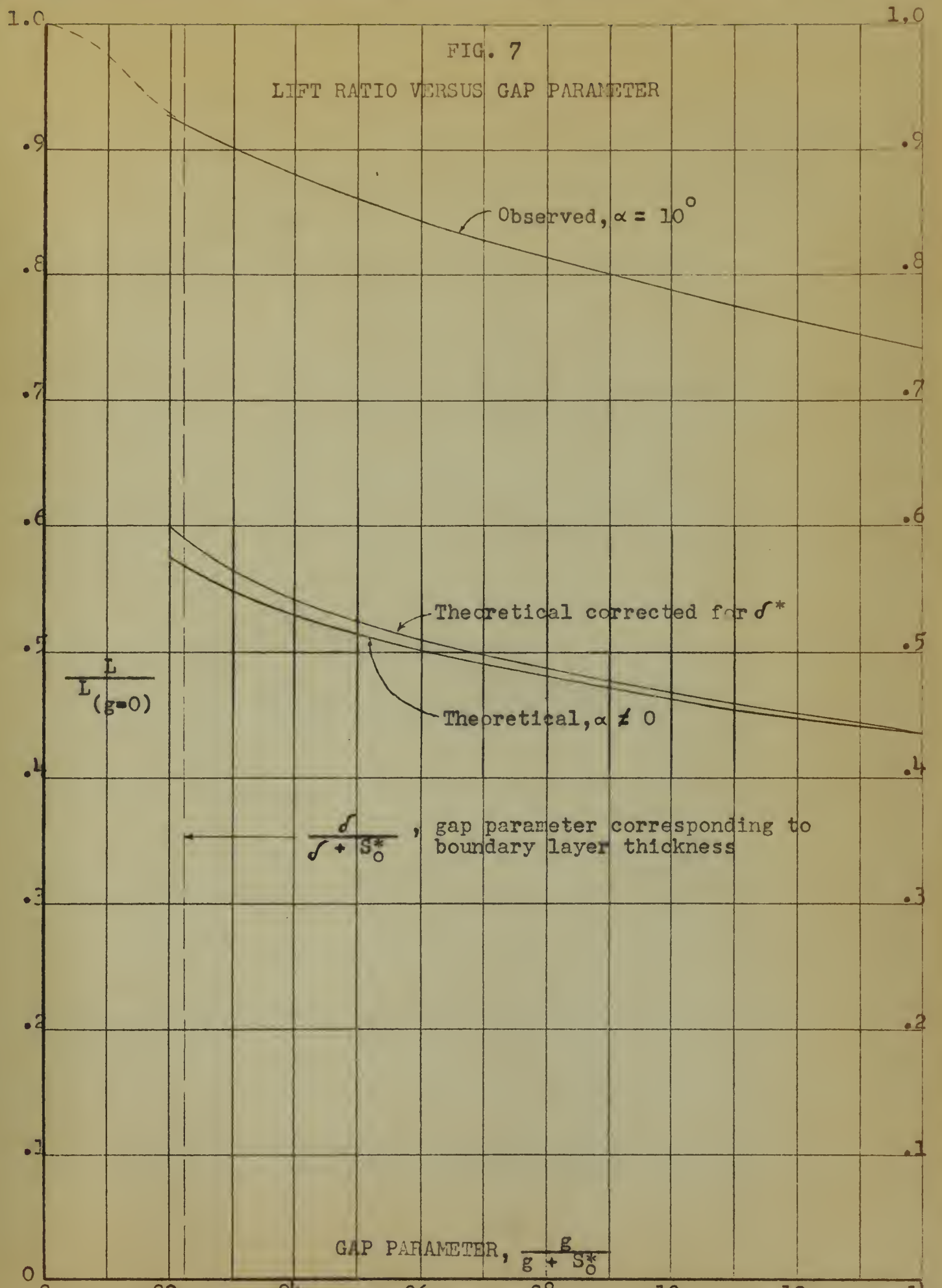

FIG. 8

PERCENTAGE INCREASE IN THEORETICAL LIFT VARIATION BY CORRECTING FOR BOUNDARY LAYER DISPLACEMENT THICKNESS COMPARED WITH THE PERCENTAGE INCREASE OF EXPERIMENT OVER THEORY

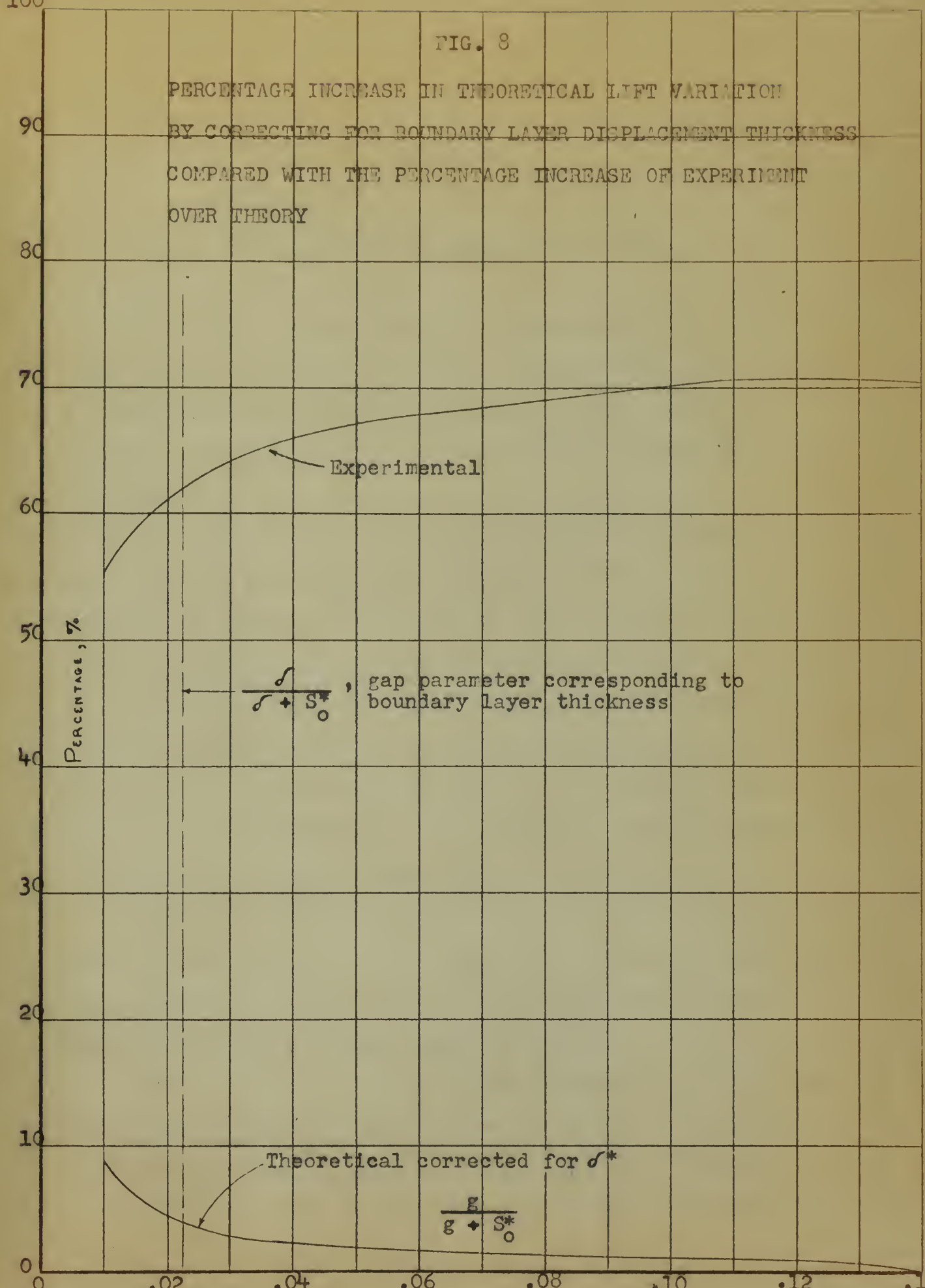

APPENDIX

NOTES ON THE FEASIBILITY OF USING A RAKE FOR BOUNDARY LAYER MEASUREMENTS

For total head measurements of thick boundary layers, such as those found on the walls of wind tunnels, etc., some investigators have successfully used a "rake", consisting of several total head probes stacked vertically with a space between them.

The possibility of interference effects in supersonic flows and the magnification of probe effects themselves are obvious. However, it was felt that the economy of runs which could be obtained with a rake warranted investigation to see if the accuracy obtained would be acceptable for this investigation. Hence a rake was constructed consisting of six probes, each similar in construction to the single probe used in the investigation. The probes were stacked together and soldered as shown in Fig. A-1.

Measurements were made with the rake in the boundary layer and free stream of the $\frac{1}{4}$ inch by $\frac{1}{4}$ inch wind tunnel at Mach number 1.9. These readings were then checked against measurements with a single total head probe.

Part of this data is tabulated in Table A-I. This data was taken during a run with the rake centered in the free stream of the tunnel. It can be seen that the outer two probes read two inches of mercury higher than the center two,

with the latter more closely checking with the single probe measurements. The boundary layer measurements likewise registered errors in the order of 5 to 13%. On this basis, the idea of using a rake was discarded in favor of the single probe.

FIG. A-1

RAKE FOR BOUNDARY LAYER MEASUREMENTS

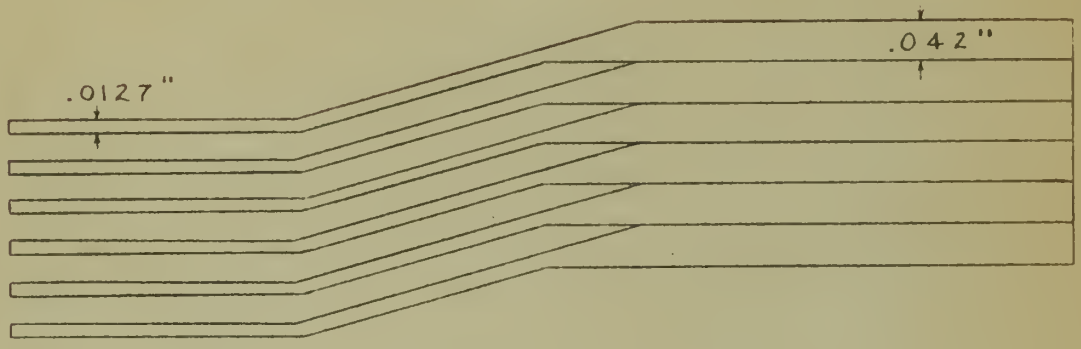

TABLE A-I

RAKE AND SINGLE PROBE READINGS COMPARED IN A FREE STREAM AT MACH NUMBER 1.9

RAKE PROBE NO.	READING in. Hg	SINGLE PROBE READING in. Hg
1	37.42	35.57
2	35.93	35.57
3	35.52	35.57
4	35.46	35.57
5	35.98	35.57
6	37.43	35.57